Published in final edited form as:
J Neurochem. 2011 April ; 117(1): 48–60. doi:10.1111/j.1471-4159.2011.07169.x.

Growth cone morphology and spreading are regulated by a dynamin–cortactin complex at point contacts in hippocampal neurons

Svetlana Kurklinsky[*], **Jing Chen**[†], and **Mark A. McNiven**[†]

[*]Mayo Graduate School, The Molecular Neuroscience Program, Rochester, Minnesota, USA

[†]Department of Biochemistry and Molecular Biology and the Center for Basic Research in Digestive Diseases, Rochester, Minnesota, USA

Abstract

Neuronal growth cone (GC) migration and targeting are essential processes for the formation of a neural network during embryonic development. Currently, the mechanisms that support directed motility of GCs are not fully defined. The large GTPase dynamin and an interacting actin-binding protein, cortactin, have been localized to GCs, although the function performed by this complex is unclear. We have found that cortactin and the ubiquitous form of dynamin (Dyn) 2 exhibit a striking co-localization at the base of the transition zone of advancing GCs of embryonic hippocampal neurons. Confocal and total internal reflection fluorescence microscopies demonstrate that this basal localization represents point contacts. Exogenous expression of wild-type Dyn2 and cortactin leads to large, exceptionally flat, and static GCs, whereas disrupting this complex has no such effect. We find that excessive GC spreading is induced by Dyn2 and cortactin over-expression and substantial recruitment of the point contact-associated, actin-binding protein α-actinin1 to the ventral GC membrane. The distributions of other point contact proteins such as vinculin or paxillin appear unchanged. Immunoprecipitation experiments show that both Dyn2 and cortactin reside in a complex with α-actinin1. These findings provide new insights into the role of Dyn2 and the actin cytoskeleton in GC adhesion and motility.

Keywords

actin; actinin; cortactin; dynamin; growth cone; hippocampus

Address correspondence and reprint requests to Mark A. McNiven, Mayo Clinic, Department of Biochemistry and Molecular Biology, 200 First Street SW, Guggenheim 1637, Rochester, MN 55905, USA. mcniven.mark@mayo.edu.

Supporting information

Additional Supporting information may be found in the online version of this article:

Movie 1. DIC movie of a GC of a DIV6 untransfected neuron.

Movie 2. DIC movie of a GC of a DIV6 neuron transfected to express Dyn2-GFP.

Movie 3. DIC movie of a GC of a DIV6 neuron transfected to express Cort-dsRED.

Movie 4. DIC movie of a GC of a DIV6 neuron transfected to express Dyn2ΔPRD-GFP.

Movie 5. DIC movie of a GC of a DIV6 neuron transfected to express CortΔSH3-dsRED.

Movie 6. Confocal microscopic 3D rotations of DIV6 GCs co-stained for Dyn2 and F-actin (phalloidin), still image in Figure 5a.

Movie 7. Confocal microscopic 3D reconstruction of DIV6 GCs co-stained for cortactin and F-actin (phalloidin), still image in Figure 5b.

As a service to our authors and readers, this journal provides supporting information supplied by the authors. Such materials are peer-reviewed and may be re-organized for online delivery, but are not copy-edited or typeset. Technical support issues arising from supporting information (other than missing files) should be addressed to the authors.

The growth cone (GC) is a highly dynamic structure found at the tips of axons. It exhibits directed motility that is essential during neuronal development and regeneration and is believed to be supported by an elaborate actin cytoskeletal meshwork (Hughes 1953; Nakai 1956; Yamada *et al.* 1970, 1971) that contributes to GC morphology and motility. Actin filaments are predominantly concentrated in the peripheral (P) and transitional (T) zones of the GCs, where the dynamics of these structures are highly regulated. The regulation of actin assembly and dynamics is controlled, in part, by an Arp2/3 complex in the lamellipodia of rat fibroblasts (Korobova and Svitkina 2008). However, this process in GCs is not well elucidated because neither Neural Wiskott-Aldrich syndrome protein (N-WASP) (Stradal *et al.* 2004) nor the Arp2/3 complex appears to be essential for actin reorganization of GC lamellipodia (Strasser *et al.* 2004; Gomez *et al.* 2007).

Several studies have implicated the large GTPase dynamin2 (Dyn2) and the associated actin-binding protein cortactin in the formation of branched actin networks within extending lamellipodia generated in epithelial cells by the Arp2/3 and Neural Wiskott-Aldrich syndrome protein (N-WASP) complex (Ochoa *et al.* 2000; Weaver *et al.* 2001; Schafer *et al.* 2002; Mooren *et al.* 2009). In addition to directly binding Arp2/3, cortactin is believed to provide a link between the actin cytoskeleton and the membrane-deforming machinery via a direct interaction with Dyn2 (McNiven *et al.* 2000b). Cortactin binds to the proline-rich domain (PRD) of Dyn2 via its C-terminal src homology-3 (SH3) domain to support a variety of cellular processes that require membrane tubulation and vesiculation, such as the liberation of endocytic and secretory vesicles from the cell surface and from the Golgi apparatus, respectively (Hinshaw 2000; McNiven *et al.* 2000a; Sever 2002; McNiven and Thompson 2006).

The conventional dynamin family is represented by three distinct gene isoforms that are expressed in a tissue-specific manner. Dyn1 is expressed in the brain (Shpetner and Vallee 1989; Cao *et al.* 1998), Dyn2 is ubiquitously expressed (Cook *et al.* 1994), and Dyn3 is expressed in a subset of tissues, including the brain (Nakata *et al.* 1993). All of the dynamin proteins are expressed as alternatively spliced forms that together could exceed 30 isoforms in neuronal tissues. Although the functions of the isoforms remain to be determined, there is substantial evidence implicating Dyn1 in synaptic vesicle recycling (Okamoto *et al.* 2001; Yamashita *et al.* 2005), whereas specific spliced forms of Dyn3 have been linked to post-synaptic morphogenesis (Gray *et al.* 2003; Lu *et al.* 2007). Currently, the specific functions of Dyn2 in neurons are unclear.

In the present study, we observed that both Dyn2 and cortactin are significantly enriched in migrating GCs of rat neonatal hippocampal neurons. Cortactin has been localized to GCs by others (Du *et al.* 1998; Ruthel and Banker 1998; Korobova and Svitkina 2008; Decourt *et al.* 2009; Mingorance-Le Meur and O'Connor 2009), although its precise localization and function have not been studied in depth. Interestingly, both cortactin and Dyn2 appear as highly enriched, punctate structures in filopodia and within the transitional zone of GCs. Moreover, we found that Dyn2 is the major dynamin form in the GC, and alterations in the expression levels of either cortactin or Dyn2 led to dramatic changes in GC length, area, dynamics, and attachment. High levels of expression of either protein resulted in well-spread and exceptionally well-attached GCs that were markedly static. In contrast, expression of truncated mutants led to long, thin axons with small, motile GCs. Confocal and total internal reflection fluorescence (TIRF) microscopies revealed that Dyn2 and cortactin associate at point contacts in the transition zone at the cell base, as confirmed by co-staining with vinculin, paxillin, and α-actinin1. Interestingly, the expression levels of Dyn2 and cortactin have direct effects on the recruitment of α-actinin1 to the base of the GC, resulting in the formation of a large α-actinin1 meshwork along the ventral membrane. In contrast, expression of the Dyn2 and cortactin truncation mutants prevented the formation of an α-

actinin1 meshwork. Co-immunoprecipitation (IP) experiments showed that Dyn2-cortactin and α-actinin1 all associate together in a complex. Thus, Dyn2 and cortactin levels directly correlate with the formation of a complex that has profound effects on GC shape, adhesion, and motility.

Experimental procedures

Cell culture and transfections

Neurons were extracted from the hippocampii of E18 Sprague–Dawley rats as previously described (Gray *et al.* 2003) and grown in Neurobasal media (Invitrogen Corporation, Carlsbad, CA, USA) supplemented with B27 (Invitrogen Corporation), 500 μM glutamine, and 1% Pen/Strep. Neurons were plated on poly-ʟ-lysine (Sigma Aldrich, St. Louis, MO, USA)-coated glass coverslips at a density of 5000 cells/cm^2, except in motility experiments, where a density of 2500 cells/cm^2 was used. 24 h post-transfection, neurons at 4–6 days *in vitro* were fixed with 4% paraformaldehyde for immunofluorescence. The transfection reagent used for hippocampal neurons was Lipo 2000 (Invitrogen Corporation) supplemented with Optimem (Invitrogen Corporation) and Nupherin (Biomol International, Plymouth Meeting, PA, USA), per the manufacturers' instructions. HeLa cells and rat fibroblasts (FRs) were acquired from American Type Culture Collection (ATCC, Rockville, MD, USA) and maintained in Dulbecco's modified Eagle's medium supplemented with 10% (FBS) (Invitrogen Corporation), 100 U/mL penicillin, and 100 μg/mL streptomycin. HeLa and FR cells were transfected using Lipofectamine and Plus reagent (Invitrogen Corporation), as suggested by the manufacturer. Transfection rates were 3–5% for hippocampal neurons and near 50% for FR and HeLa cells.

Microscopy and immunofluorescence

Neurons were fixed for 20 min in pre-warmed 4% paraformalde-hyde in phosphate-buffered saline (PBS) (Strasser *et al.* 2004) at 37 °C, with all subsequent steps performed at 22 °C. Following fixation, neurons were permeabilized with 0.001% Digitonin for 2 min, then placed in blocking buffer (5% goat serum, 5% glycerol, 0.04% sodium azide in d-PBS) for 1 h. Primary antibodies were diluted in a blocking buffer solution and were incubated with the cells for 2–3 h. Following extensive washing, samples were incubated with fluorophore-conjugated secondary antibodies for 1 h. ProLongGold (Invitrogen Corporation) anti-fade reagent was used as a mounting medium for epifluorescence and confocal microscopy. For TIRF microscopy, Fluoromount-G (Southern Biotech, Birmingham, AL, USA) was the anti-fade reagent.

For indirect immunocytochemistry, FRs were fixed and permeabilized with PBS containing 0.1% Triton X-100 for 2 min and incubated with antibodies as described previously (Henley and McNiven 1996). For F-actin localization, rhodamine-phalloidin (Sigma Aldrich) was included in both the primary and secondary antibody steps.

Live imaging experiments were performed using either perfusion chambers or gridded imaging dishes (both made at the engineering division at Mayo Clinic). Differential interference contrast microscopy was utilized to visualize live neurons. Images were captured using a Zeiss Axiovert 200 epifluorescent microscope (Carl Zeiss, Inc., Thornwood, NJ, USA) with an Orca II cooled-CCD camera (Hamamatsu Photonics, Hamamatsu City, Japan) and the BioVision software program (previously called IPLab) (BioVision, Mountain View, CA, USA). Images were captured every 3 s to generate movies and subsequent kymographs. Images from kymographs represent regions of 100 × 6 pixels of lamellipodia or filopodia in GCs from the regions indicated by arrows in Fig. 4. Confocal microscopy was performed using a Carl Zeiss LSM-510 with plan-Apochromat 63× NA1.4

lens (Carl Zeiss, Inc.) equipped with an argon-krypton laser. TIRF microscopy was performed using an Axiovert 200M (Carl Zeiss, Inc.) with a module for TIRF and a plan-Apochromat 100× NA1.4 lens.

To compare and quantitate the levels of exogenously expressed, versus endogenous, protein levels, cultured cells were transfected to express fluorescently-tagged proteins of interest, then were subsequently fixed and labeled for immunofluorescence using an antibody to the expressed protein. Intensity levels of transfected versus the surrounding untransfected cells were then measured to calculate a ratio utilizing BioVision software (BioVision).

Western blot analysis and immunoprecipitation

RF/HeLa cells were grown on 150-mm dishes in Dulbecco's modified Eagle's medium supplemented with 10% newborn calf serum. To test the specificities of the three dynamin peptide polyclonal antibodies used in this study, HeLa cells were transfected to over-express the green fluorescent protein (GFP)-tagged forms of Dyn1, Dyn2, or Dyn3. In IP experiments, FR cells were transfected with Dyn2-GFP, Dyn2ΔPRD-GFP, Cort-Discosoma sp. red fluorescent protein (ds-RED), or CortΔSH3-dsRED. After 24 h of expression, the transfected cells were lysed and harvested in ice-cold hypotonic lysis buffer (10 mM Tris–HCl, pH 7.5, 10 mM NaCl, 5 mM $MgCl_2$, 0.2 mM EDTA, 1 mM sodium orthovanadate, and 40 mM ammonium molybdate) and then supplemented with complete protease inhibitor tablets (Roche Diagnostics, Basel, Switzerland). Protein A or G sepharose beads (Invitrogen Corporation, Eugene, OR, USA) were used for precipitation of proteins bound to specific antibodies from these lysates. Following a wash with lysis buffer, beads were boiled at 100 °C for 3 min and analyzed by sodium dodecyl sulfate-polyacrylamide gel electrophoresis.

Measurement of axonal GC area, axonal length, and co-localization

Growth cone size and axonal length were measured utilizing BioVision software (BioVision). In the case of axonal length, we traced axons that were either expressing fluorescent protein of interest or in the case of control we used tau stain for visualization. GC size was measured by tracing GCs that were expressing protein of interest or fluorescently labeled with Dyn2 or cortactin. In each experiment, axonal length and GC size was measured in 120–200 neurons per condition. JMP software (SAS Campus Drive, Cary, NC, USA) was used for ANOVA statistical analyses.

Overlap of Dyn2 and cortactin within GCs in Fig. 1 was measured using a co-localization module from BioVision software (BioVision). Areas of interest were outlined, and Pearson's correlation coefficient was used to quantitate and compare co-localization in the filopodia, lamellipodia, and transitional zone to co-localization in the central area. More than 80 GCs were examined for co-localization calculation.

For calculation of a co-localization coefficient (Fig. 5), images were captured using Zeiss Axiovert 200 epifluorescence microscope (Carl Zeiss, Inc.) and exported into LSM 510 software (Carl Zeiss, Inc.). Areas of interest were outlined, and the levels of co-localization between red and green channels representing each protein of interest residing within the growth cone P and C domain were calculated by the Zeiss software. Twenty GCs were examined for each protein co-localization calculation.

Constructs

Generation of the Dyn2-GFP construct was described previously (Cao *et al.* 1998; Jones *et al.* 1998). The Dyn2ΔPRD-GFP, Cort-dsRED, and CortΔSH3-dsRED constructs were published previously (McNiven *et al.* 2000b), whereas Cort-GFP and CortΔSH3-GFP were re-cloned from the dsRED vector into a GFP vector, while Dyn2-dsRED, Dyn2ΔPRD-

dsRED, and Cort-dsRED were re-cloned from the GFP vector into a dsRED vector, using constructs that were previously published. α-actinin1-GFP was purchased (Addgene, Cambridge, MA, USA).

Antibodies

Antibodies developed in our laboratory and previously published include the following: anti-Dyn1, Pan MC63 (Henley and McNiven 1996), anti-Dyn2 (Cook *et al.* 1994), anti-Dyn3 (Cao *et al.* 1998), anti-cortactin AB3, and anti-cortactin C-Tyr (Cao *et al.* 2003). Purchased antibodies include anti-cortactin (Millipore corporation, Billerica, MA, USA), anti-α-actinin1 (Santa Cruz Biotechnology, Inc., Santa Cruz, CA, USA; Sigma Aldrich), anti-tau (BD, Franklin Lakes, NJ, USA), anti-vinculin (Sigma Aldrich), anti-paxillin (BD), anti-GFP (Roche Diagnostics), and anti-dsRED (Clontech Laboratories, Inc., Mountain View, CA, USA). Goat anti-rabbit or goat anti-mouse secondary antibodies conjugated to Alexa 488 or 594 were from Invitrogen Corporation. Secondary antibodies used for TIRF microscopy were the following: TRITC (Zymed Laboratories, Inc., San Francisco, CA, USA), Alexa 430 (Invitrogen Corporation), and Alexa 488 (Invitrogen Corporation).

Results

Dyn2 and cortactin co-localize at the transitional zone of hippocampal GCs

Because Dyn2 and cortactin have been implicated in lamellipodial extension and cell motility in many epithelial cell types (McNiven *et al.* 2000b), we tested if these proteins might have a similar role in GC motility. Immunofluorescence staining of hippocampal neurons for Dyn2 and cortactin showed substantial, almost exact co-localization in the transitional zone of migrating GCs (Fig. 1a–d"). As observed by phase-digital imaging, this region of co-localization corresponded to the base of the filopodia in the transitional zone of GCs (Fig. 1b and b'). Some Dyn2 staining was observed along the length of the axonal shaft and in the GC central domain, as well, but this staining was significantly less than the level observed at the tip of the GC.

The conventional dynamin family consists of three related isoforms (Dyn1, 2, and 3) that are expressed in a tissue-specific manner (Shpetner and Vallee 1989; Nakata *et al.* 1993; Cook *et al.* 1994; Cao *et al.* 1998). Because all three forms are expressed in the brain, we examined which dynamin isoform(s) are localized to the GC (Fig. 1a–f). Use of isoform-specific antibodies (Cao *et al.* 1998) and subsequent staining of cultured neurons show little, if any, localization of Dyn1 or Dyn3 in GCs (Fig. 1e and f). To define the specificity of these antibody reagents, we exogenously expressed Dyn1-GFP, Dyn2-GFP, and Dyn3-GFP in HeLa cells and then performed western blot analysis with each antibody to test for cross-reactivity (Fig. 1g). The neoplastic HeLa cells express endogenous forms of Dyn2 in addition to some Dyn3, as observed by others (Liu *et al.* 2008). Importantly, the Dyn2 and Dyn3 antibodies recognized only their respective antigens, although the Dyn1 antibody reacted weakly with Dyn2. As the Dyn1 and Dyn3 proteins were only modestly detected in GCs, we conclude that Dyn2 is the predominant form in the GCs of hippocampal neurons.

Expression of Dyn2 and cortactin controls GC size, spreading, and motility

How Dyn2 and cortactin contribute to GC migration and extension is currently unclear. Days *in vitro* 5 hippocampal neurons were transfected to express Dyn2-GFP or Cort-dsRED, then fixed and stained 24 h post-expression. Levels of exogenously expressed proteins were 4–5 times higher then endogenous levels of proteins as compared with adjacent untransfected cells stained with the same antibodies. Interestingly, GCs expressing either of these proteins individually exhibited a remarkable increase in size, becoming substantially more spread out, with punctate Dyn2/cortactin spots decorating mostly the transitional zone

(Fig. 2a–f). GCs stained for endogenous Dyn2/cortactin showed localization at the transitional zone and some in the filopodia. Over-expression of Dyn2/cortactin resulted in expansion of 'hot spot' areas in the transitional zone, with localization of both Dyn2 and cortactin in the central domain, as well. Morphometric quantitation of GC area showed an increase in size of 57% and 59% for Dyn2-GFP- and Cort-dsRED-expressing cells, respectively (Fig. 2g), suggesting that these proteins contribute to the attachment and spreading of neuronal GCs. Axonal length measurements demonstrated that neurons transfected with Dyn2-GFP or Cort-RFP had axons of comparable lengths to controls (Fig. 2h).

To test whether the interaction of Dyn2 and cortactin might have functional effects on GC morphology, truncated versions of these proteins that lack the interactive PRD and SH3 domains, respectively, were expressed (Grabs *et al.* 1997; McNiven *et al.* 2000b). Expression of these truncated proteins induced the growth of exceptionally long axons (Fig. 3f, g and h) and small GCs with extending filopodia and a motile phenotype (Fig. 3b and c and Movies S4 and S5). Morphometric quantitation showed a 73% and 74% decrease in GC area in DynΔPRD-GFP- and CortΔSH3-dsRED-expressing cells, respectively (Fig. 3d), and a 50% and 39% increase in axonal length compared with control neurons (Fig. 3h). Thus, when GC area is compared between neurons expressing wild-type (wt) Dyn2/cortactin versus the truncated non-interactive forms, there is a 500% change in the size of these GCs in a 24-h period. This result strongly suggests that the complex plays an important role in the spreading size and dynamics of neuronal extensions.

To test if increased levels of Dyn2/cortactin might exert a functional effect on GC dynamics, differential interference contrast-digital images of neurons expressing either full-length or truncated Dyn2 and cortactin were collected every 6 s for a period of 5 min and displayed as kymographs to provide a qualitative depiction of membrane ruffling (Fig. 4a'–e'). GCs expressing full-length Dyn2 and cortactin became exceptionally flattened and completely static and exhibited virtually no ruffling or treadmilling of the peripheral membrane (Fig. 4b and c and Movies S2 and S3) when compared to control neurons (Fig. 4a and Movie S1). In contrast, neurons expressing the truncated mutant proteins acquired filopodial morphology (Fig. 4d and e) and exhibited increased dynamics, as demonstrated by kymograph analysis (Fig. 4a'–e'). Kymographs were quantified by calculating the average slopes of GC ruffles (Fig. 4f–f'), which confirmed a dramatic change in GC dynamics in control and mutant-expressing cells compared with cells expressing high levels of wt proteins (Fig. 4g). It is worth noting that cells expressing the truncated mutant proteins appeared more stressed than untransfected neurons. This observation might not be surprising, given that cortactin and Dyn2 participate in a variety of cellular functions. Despite this stress, it is impressive that the neurons maintained long, motile GCs.

Dyn2 and cortactin localize to adhesion sites in extending GCs to form a complex with α-actinin1

From the images displayed in Figs 1-3, it appears that the Dyn2-cortactin complex is localized to discrete regions at the base of the transitional zone of the GC. This ventral localization was supported by Z-series confocal imaging of GCs stained for Dyn2, cortactin, and actin (Fig. 5a–b'), which revealed a significant proportion of total staining at the base, with lesser amounts extending upward into the filopodia. Because this punctate localization was reminiscent of point contact structures, GCs were co-stained with several adhesion markers including paxillin (Fig. 5d–d", e–e"), Focal Adhesion Kinase (FAK), vinculin, and α-actinin1 (data not shown). Co-localization of Dyn2 and cortactin with paxillin was the most substantial in the P domain of the GC (Fig. 5d"', e"'), where 92% of cortactin and 86% of Dyn2 co-localized with paxillin. Less co-localization of these proteins was observed in the C zone where 22% of cortactin and 31% of Dyn2 co-localized with paxillin. It is

important to note that most (62%) of the paxillin was localized in the P zone, a region that represents just 10% of the total GC area. Similar accumulations were observed for Dyn2 (74%) and cortactin (70%) in the GC P domain.

Cells were viewed using a Zeiss TIRF microscope to facilitate imaging of 100–200 nm into the cell base. From these images we observed significant co-localization of Dyn2 and cortactin (Fig. 5c–c”’) strengthening the notion that these proteins reside at GC point contacts.

Most striking was the change in the distribution of α-actinin1 in GCs upon over-expression of either Dyn2 or cortactin, which induced the formation of exceptionally large, flat, and static GCs (Figs 2 and 4). Standard epifluorescence or confocal microscopy showed only modest changes in the distribution of α-actinin1 in these neurons (data not shown). In contrast, TIRF microscopy revealed that these flat GCs expressing either Cort-dsRED (Fig. 6b–b”) or Dyn2-dsRED (Fig. 6e–e”) underwent a dramatic redistribution of endogenous α-actinin1, which was observed as a broad accumulation covering most of the very ventral membrane in an intricate web-like morphology (Fig. 6b”, e”). Over-expression of truncated mutant versions of Dyn2 and cortactin that lacked the interactive PRD or SH3 domains, respectively, did not result in ventral recruitment of endogenous α-actinin1 but, rather, a reduction of total α-actinin1 (Fig. 6c”, f”).

Similar effects were observed in FRs, which were utilized to better analyze adhesion sites. In these cells, co-expression of Cort-dsRED and α-actinin1-GFP, or Dyn2-dsRED and α-actinin1-GFP, induced the formation of a very bright α-actinin1 meshwork along the base of the cell (Fig. 7b and c). Importantly, co-expression of α-actinin1-GFP and the truncated mutants of Dyn2 or cortactin did not lead to α-actinin1 recruitment at the cell base but instead resulted in modest-sized focal adhesions (Fig. 7d and e).

To provide a biochemical correlation with the morphological changes described above, we tested for interactions between cortactin, Dyn2, and α-actinin1 in FR cell lysates by using a co-IP approach. Importantly, these IP experiments revealed substantial interactions among Dyn2, cortactin, and α-actinin1 (Fig. 7f–g). Although modest interactions with the α-actinin1-binding protein vinculin were also observed, no interaction with paxillin was detected (Fig. 7f). Using the same approach, we tested if truncated versions of Dyn2 and cortactin, expressed in FRs and lacking the interactive PRD and SH3 domains, respectively, would exhibit reduced interactions with each other and with α-actinin1. As expected, the expressed Dyn2ΔPRD protein was not pulled down by the cortactin IP (Fig. 7h). Importantly, this truncated protein did not associate with α-actinin1 by IP (Fig. 7i), suggesting that the Dyn2 PRD mediates either direct binding of α-actinin1 or an indirect interaction via cortactin or other proteins. In contrast, IP of α-actinin1 from cells expressing either full-length or a truncated cortactin protein (CortΔSH3) revealed that both forms bind to α-actinin1 (Fig. 7j). Thus, based on the combined morphological and biochemical observations from Figs 6 and 7, we conclude that Dyn2, cortactin, and α-actinin1 form a functional complex at the cell base that regulates GC adhesion and motility. Future detailed studies will define which of these interactions are direct and identify the specific domains in each protein that might mediate this mutual binding.

Discussion

In this study, we show that the Dyn2-cortactin complex plays a major role in GC morphology, adhesion, and dynamics. This complex appears to be largely localized to the transitional zone of advancing GCs (Fig. 1). Importantly, over-expression of this complex results in large, flat, and static GCs (Figs 2 and 4), whereas disrupting Dyn2-cortactin

interactions by the expression of truncated proteins lacking the interactive PRD and SH3 domains leads to long axons and a smaller GC area (Figs 3 and 4). TIRF microcopy confirmed that the Dyn2-cortactin complex is predominately located at the base of the GC, along with other components of point contacts (Fig. 5), which suggests why over-expression of this complex leads to exaggerated spreading and attachment. Finally, we provide evidence linking the Dyn2-cortactin complex to point contacts via an interaction with the focal adhesion-localized, actin-binding protein α-actinin1, both in GCs (Fig. 6) and in rat fibroblasts (Fig. 7).

The Dyn2 isoform as a mediator of GC dynamics

Our finding that the Dyn2 isoform mediates GC motility constitutes one of the few identified functions for this protein in neurons. Although all three of the conventional dynamins are expressed in the brain, Dyn1 and Dyn3 are believed to participate in synapse-specific functions. Dyn3 has been implicated in the regulation of actin dynamics during dendritic spine development and filopodial induction (Gray *et al.* 2003, 2005), whereas Dyn1 is found primarily in the pre-synapses, where it is required for rapid synaptic-membrane endocytosis and recycling (Takei *et al.* 1996; Shupliakov *et al.* 1997). Dyn1 has been implicated in two pathways, one that is phosphorylation-independent and essential for clathrin-dependent endocytosis, and the other that is phosphorylation-dependent and appears to sustain rapid endocytosis of bulk membranes in frog neuromuscular junctions (Liu *et al.* 1994; Richards *et al.* 2000).

Dynamin2 has been implicated in the endocytosis of receptors in neurons such as the μ-opioid (Patel *et al.* 2002), D_2 dopamine (Kabbani *et al.* 2004), and mGluR5 (Fourgeaud *et al.* 2003) receptors. Since Dyn2 is ubiquitously expressed (Cook *et al.* 1994; Sontag *et al.* 1994) and has been shown to regulate endocytic internalization in epithelial cells (Apodaca 2001), this isoform has been assumed to mediate routine ‘household’ endocytosis in neurons, while Dyn1/3 isoforms perform neuron-specific functions. There is now a wealth of observations linking Dyn2 to actin-based functions in non-neuronal cells (Orth and McNiven 2003; McNiven *et al.* 2004; Kruchten and McNiven 2006), such as the migration of epithelial cells (Krueger *et al.* 2003), actin comet formation that supports the transport of macropinosomes, and the formation of podosomes/invadopodia (Ochoa *et al.* 2000; Baldassarre *et al.* 2003). The observation that cortactin binds directly to the PRD of Dyn2 (McNiven *et al.* 2000b; Schafer *et al.* 2002) provided insights into how the dynamins might participate in these actin-based processes.

The role of the endocytic process in cell migration is not fully understood. Membrane turnover is thought to occur both at the rear of the cell, for subsequent transport to provide new membrane at the leading edge (Cheng and Reese 1987), and at the leading edge, where macropinocytosis occurs. We are unaware of any studies implicating the dynamins in this process, although one study has shown a functional inter-relationship between Dyn2 and the small GTPase Rac (Schlunck *et al.* 2004). Because both Dyn2 (Ezratty *et al.* 2005) and cortactin (Kruchten *et al.* 2008) have recently been localized to focal adhesions in epithelial cells, it has been proposed that these proteins mediate regulated endocytic uptake of these structures to support migration. The massive increased spreading and recruitment of other adhesion components in this study may also indicate that the Dyn2-cortactin complex has a structural role by recruiting additional cytoskeletal components. This complex could facilitate GC migration both by mediating extension of the filopodia and by controlling point contact dynamics. A central finding of this study is the identification of a novel functional interaction between Dyn2-cortactin and α-actinin1 that provides new insights into focal adhesion dynamics and function in both GCs and non-neuronal cells.

A novel Dyn2-cortactin-α-actinin1 complex at point contacts within GCs

The family of α-actinin proteins has been implicated in a variety of important cytoskeletal events. There are four isoforms of α-actinin, all of which have an N-terminal actin-binding domain followed by multiple spectrin repeats and two consecutive calponin homology domains. Structural interactions between α-actinin and its effectors typically occur between the negatively charged rod domain (spectrin repeats) and positively charged cytoplasmic peptides, respectively (Sjoblom *et al.* 2008). α-actinin interaction partners include vinculin (Belkin and Koteliansky 1987; Wachsstock *et al.* 1987), zyxin (Crawford *et al.* 1992), integrins (Otey *et al.* 1990), and cysteine-rich protein (Pomies *et al.* 1997), among many others.

How these interactions might alter point contacts to affect GC dynamics is unclear. Dyn2 and cortactin have been implicated in focal adhesion internalization and recycling (Ezratty *et al.* 2005; Kruchten and McNiven 2006). Therefore, over-expression of these proteins that leads to recruitment of inappropriate levels of α-actinin1 at the cell base (Figs 6 and 7) could result in hyper-stabilized adhesion structures that cannot recycle. This process would promote the formation of the observed large, abnormally spread, and static GCs (Figs 2 and 4). By disrupting this complex through the expression of truncated mutant forms (Figs 3 and 4) of Dyn2 and cortactin, α-actinin1 recruitment is minimized and point contacts become modest, leading to thin neurites and poorly spread GCs (Fig. 6). The observation that the Dyn2ΔPRD mutant does not bind to either cortactin or α-actinin1 (Fig. 7h and i) suggests that the integrity of this trimeric complex can profoundly affect the actin cytoskeleton. Why the CortΔSH3 domain mutant, which does not bind Dyn2, interacts with α-actinin1 is unclear, but this finding suggests that additional regions of cortactin, such as the 6.5 actin-binding domains, can play a role. Certainly, future detailed mapping of the precise binding domains of all three proteins will be important.

We have found that the expression levels of wt versus mutant proteins have significant effects on GC shape and dynamics. Normal endogenous levels of Dyn2/cortactin facilitate appropriate adhesion formation and turnover that support migratory growth. Over-expression of wt forms leads to an inappropriate recruitment of a Dyn2-cortactin-α-actinin1 complex to the GC substrate, resulting in massive adhesions that produce large, flat, non-motile GCs. In contrast, the expression of mutant truncated forms of Dyn2/cortactin prevents mutual binding and recruitment to the GCs. These observations extend the findings of others such as *Drosophila* where the *shibire* (*ts*) mutant inhibits neurite extension from cultured neurons (Masur *et al.* 1990) or in cultured rat hippocampal neurons where a reduction in Dyn1 by antisense oligonucleotide treatment prevents neurite formation (Torre *et al.* 1994). As this antisense treatment reduced total Dyn1 levels by over 90%, it is likely that this probe also affected Dyn2 expression significantly.

From these observations, we predict that Dyn2-cortactin plays a central structural role in focal adhesion assembly in GCs. Further study of the regulated interaction of these three proteins in neurons and non-neuronal cells will provide important insight into a variety of dynamic cellular functions.

Supplementary Material

Refer to Web version on PubMed Central for supplementary material.

Acknowledgments

The authors acknowledge the use of the Optical Microscopy Core of the Mayo Clinic Center for Cell Signaling in Gastroenterology (P30DK084567) and would like to thank Dr. Hong Cao for the use of many of his DNA constructs and for helpful advice.

Abbreviations used

ds-RED	Discosoma sp. red fluorescent protein
Dyn	dynamin
FR	rat fibroblast
GC	growth cone
GFP	The green fluorescent protein
IP	immunoprecipitation
PBS	phosphate-buffered saline
PRD	proline-rich domain
SH3	src homology-3
TIRF	total internal reflection fluorescence
wt	wild-type

References

Apodaca G. Endocytic traffic in polarized epithelial cells: role of the actin and microtubule cytoskeleton. Traffic. 2001; 2:149–159. [PubMed: 11260520]

Baldassarre M, Pompeo A, Beznoussenko G, Castaldi C, Cortellino S, McNiven MA, Luini A, Buccione R. Dynamin participates in focal extracellular matrix degradation by invasive cells. Mol. Biol. Cell. 2003; 14:1074–1084. [PubMed: 12631724]

Belkin AM, Koteliansky VE. Interaction of iodinated vinculin, metavinculin and alpha-actinin with cytoskeletal proteins. FEBS Lett. 1987; 220:291–294. [PubMed: 3111888]

Cao H, Garcia F, McNiven MA. Differential distribution of dynamin isoforms in mammalian cells. Mol. Biol. Cell. 1998; 9:2595–2609. [PubMed: 9725914]

Cao H, Orth JD, Chen J, Weller SG, Heuser JE, McNiven MA. Cortactin is a component of clathrin-coated pits and participates in receptor-mediated endocytosis. Mol. Cell. Biol. 2003; 23:2162–2170. [PubMed: 12612086]

Cheng TP, Reese TS. Recycling of plasmalemma in chick tectal growth cones. J. Neurosci. 1987; 7:1752–1759. [PubMed: 3598645]

Cook TA, Urrutia R, McNiven MA. Identification of dynamin 2, an isoform ubiquitously expressed in rat tissues. Proc. Natl Acad. Sci. USA. 1994; 91:644–648. [PubMed: 8290576]

Crawford AW, Michelsen JW, Beckerle MC. An interaction between zyxin and alpha-actinin. J. Cell Biol. 1992; 116:1381–1393. [PubMed: 1541635]

Decourt B, Munnamalai V, Lee AC, Sanchez L, Suter DM. Cortactin colocalizes with filopodial actin and accumulates at IgCAM adhesion sites in Aplysia growth cones. J. Neurosci. Res. 2009; 87:1057–1068. [PubMed: 19021290]

Du Y, Weed SA, Xiong WC, Marshall TD, Parsons JT. Identification of a novel cortactin SH3 domain-binding protein and its localization to growth cones of cultured neurons. Mol. Cell. Biol. 1998; 18:5838–5851. [PubMed: 9742101]

Ezratty EJ, Partridge MA, Gundersen GG. Microtubule-induced focal adhesion disassembly is mediated by dynamin and focal adhesion kinase. Nat. Cell Biol. 2005; 7:581–590. [PubMed: 15895076]

Fourgeaud L, Bessis AS, Rossignol F, Pin JP, Olivo-Marin JC, Hemar A. The metabotropic glutamate receptor mGluR5 is endocytosed by a clathrin-independent pathway. J. Biol. Chem. 2003; 278:12222–12230. [PubMed: 12529370]

Gomez TS, Kumar K, Medeiros RB, Shimizu Y, Leibson PJ, Billadeau DD. Formins regulate the actin-related protein 2/3 complex-independent polarization of the centrosome to the immunological synapse. Immunity. 2007; 26:177–190. [PubMed: 17306570]

Grabs D, Slepnev VI, Songyang Z, David C, Lynch M, Cantley LC, De Camilli P. The SH3 domain of amphiphysin binds the proline-rich domain of dynamin at a single site that defines a new SH3 binding consensus sequence. J. Biol. Chem. 1997; 272:13419–13425. [PubMed: 9148966]

Gray NW, Fourgeaud L, Huang B, Chen J, Cao H, Oswald BJ, Hemar A, McNiven MA. Dynamin 3 is a component of the postsynapse, where it interacts with mGluR5 and Homer. Curr. Biol. 2003; 13:510–515. [PubMed: 12646135]

Gray NW, Kruchten AE, Chen J, McNiven MA. A dynamin-3 spliced variant modulates the actin/cortactin-dependent morphogenesis of dendritic spines. J. Cell Sci. 2005; 118:1279–1290. [PubMed: 15741233]

Henley JR, McNiven MA. Association of a dynamin-like protein with the Golgi apparatus in mammalian cells. J. Cell Biol. 1996; 133:761–775. [PubMed: 8666662]

Hinshaw JE. Dynamin and its role in membrane fission. Annu. Rev. Cell Dev. Biol. 2000; 16:483–519. [PubMed: 11031245]

Hughes A. The growth of embryonic neurites; a study of cultures of chick neural tissues. J. Anat. 1953; 87:150–162. [PubMed: 13044726]

Jones SM, Howell KE, Henley JR, Cao H, McNiven MA. Role of dynamin in the formation of transport vesicles from the trans-Golgi network. Science. 1998; 279:573–577. [PubMed: 9438853]

Kabbani N, Jeromin A, Levenson R. Dynamin-2 associates with the dopamine receptor signalplex and regulates internalization of activated D2 receptors. Cell. Signal. 2004; 16:497–503. [PubMed: 14709338]

Korobova F, Svitkina T. Arp2/3 complex is important for filopodia formation, growth cone motility, and neuritogenesis in neuronal cells. Mol. Biol. Cell. 2008; 19:1561–1574. [PubMed: 18256280]

Kruchten AE, McNiven MA. Dynamin as a mover and pincher during cell migration and invasion. J. Cell Sci. 2006; 119:1683–1690. [PubMed: 16636070]

Kruchten AE, Krueger EW, Wang Y, McNiven MA. Distinct phospho-forms of cortactin differentially regulate actin polymerization and focal adhesions. Am. J. Physiol. Cell Physiol. 2008; 295:C1113–C1122. [PubMed: 18768925]

Krueger EW, Orth JD, Cao H, McNiven MA. A dynamin-cortactin-Arp2/3 complex mediates actin reorganization in growth factor-stimulated cells. Mol. Biol. Cell. 2003; 14:1085–1096. [PubMed: 12631725]

Liu JP, Sim AT, Robinson PJ. Calcineurin inhibition of dynamin I GTPase activity coupled to nerve terminal depolarization. Science. 1994; 265:970–973. [PubMed: 8052858]

Liu YW, Surka MC, Schroeter T, Lukiyanchuk V, Schmid SL. Isoform and splice-variant specific functions of dynamin-2 revealed by analysis of conditional knock-out cells. Mol. Biol. Cell. 2008; 19:5347–5359. [PubMed: 18923138]

Lu J, Helton TD, Blanpied TA, Racz B, Newpher TM, Weinberg RJ, Ehlers MD. Postsynaptic positioning of endocytic zones and AMPA receptor cycling by physical coupling of dynamin-3 to Homer. Neuron. 2007; 55:874–889. [PubMed: 17880892]

Masur SK, Kim YT, Wu CF. Reversible inhibition of endocytosis in cultured neurons from the Drosophila temperature-sensitive mutant shibirets1. J. Neurogenet. 1990; 6:191–206. [PubMed: 2113575]

McNiven MA, Thompson HM. Vesicle formation at the plasma membrane and trans-Golgi network: the same but different. Science. 2006; 313:1591–1594. [PubMed: 16973870]

McNiven MA, Cao H, Pitts KR, Yoon Y. The dynamin family of mechanoenzymes: pinching in new places. Trends Biochem. Sci. 2000a; 25:115–120. [PubMed: 10694881]

McNiven MA, Kim L, Krueger EW, Orth JD, Cao H, Wong TW. Regulated interactions between dynamin and the actin-binding protein cortactin modulate cell shape. J. Cell Biol. 2000b; 151:187–198. [PubMed: 11018064]

McNiven MA, Baldassarre M, Buccione R. The role of dynamin in the assembly and function of podosomes and invado-podia. Front. Biosci. 2004; 9:1944–1953. [PubMed: 14977600]

Mingorance-Le Meur A, O'Connor TP. Neurite consolidation is an active process requiring constant repression of protrusive activity. EMBO J. 2009; 28:248–260. [PubMed: 19096364]

Mooren OL, Kotova TI, Moore AJ, Schafer DA. Dynamin2 GTPase and cortactin remodel actin filaments. J. Biol. Chem. 2009; 284:23995–24005. [PubMed: 19605363]

Nakai J. Dissociated dorsal root ganglia in tissue culture. Am. J. Anat. 1956; 99:81–129. [PubMed: 13362126]

Nakata T, Takemura R, Hirokawa N. A novel member of the dynamin family of GTP-binding proteins is expressed specifically in the testis. J. Cell Sci. 1993; 105(Pt 1):1–5. [PubMed: 8360266]

Ochoa GC, Slepnev VI, Neff L, et al. A functional link between dynamin and the actin cytoskeleton at podosomes. J. Cell Biol. 2000; 150:377–389. [PubMed: 10908579]

Okamoto PM, Gamby C, Wells D, Fallon J, Vallee RB. Dynamin isoform-specific interaction with the shank/ProSAP scaffolding proteins of the postsynaptic density and actin cytoskeleton. J. Biol. Chem. 2001; 276:48458–48465. [PubMed: 11583995]

Orth JD, McNiven MA. Dynamin at the actin-membrane interface. Curr. Opin. Cell Biol. 2003; 15:31–39. [PubMed: 12517701]

Otey CA, Pavalko FM, Burridge K. An interaction between alpha-actinin and the beta 1 integrin subunit in vitro. J. Cell Biol. 1990; 111:721–729. [PubMed: 2116421]

Patel M, Gomes B, Patel C, Yoburn BC. Antagonist-induced micro-opioid receptor up-regulation decreases G-protein receptor kinase-2 and dynamin-2 abundance in mouse spinal cord. Eur. J. Pharmacol. 2002; 446:37–42. [PubMed: 12098583]

Pomies P, Louis HA, Beckerle MC. CRP1, a LIM domain protein implicated in muscle differentiation, interacts with alpha-actinin. J. Cell Biol. 1997; 139:157–168. [PubMed: 9314536]

Richards DA, Guatimosim C, Betz WJ. Two endocytic recycling routes selectively fill two vesicle pools in frog motor nerve terminals. Neuron. 2000; 27:551–559. [PubMed: 11055437]

Ruthel G, Banker G. Actin-dependent anterograde movement of growth-cone-like structures along growing hippocampal axons: a novel form of axonal transport? Cell Motil. Cytoskeleton. 1998; 40:160–173. [PubMed: 9634213]

Schafer DA, Weed SA, Binns D, Karginov AV, Parsons JT, Cooper JA. Dynamin2 and cortactin regulate actin assembly and filament organization. Curr. Biol. 2002; 12:1852–1857. [PubMed: 12419186]

Schlunck G, Damke H, Kiosses WB, Rusk N, Symons MH, Waterman-Storer CM, Schmid SL, Schwartz MA. Modulation of Rac localization and function by dynamin. Mol. Biol. Cell. 2004; 15:256–267. [PubMed: 14617821]

Sever S. Dynamin and endocytosis. Curr. Opin. Cell Biol. 2002; 14:463–467. [PubMed: 12383797]

Shpetner HS, Vallee RB. Identification of dynamin, a novel mechanochemical enzyme that mediates interactions between microtubules. Cell. 1989; 59:421–432. [PubMed: 2529977]

Shupliakov O, Low P, Grabs D, Gad H, Chen H, David C, Takei K, De Camilli P, Brodin L. Synaptic vesicle endocytosis impaired by disruption of dynamin-SH3 domain interactions. Science. 1997; 276:259–263. [PubMed: 9092476]

Sjoblom B, Salmazo A, Djinovic-Carugo K. Alpha-actinin structure and regulation. Cell. Mol. Life Sci. 2008; 65:2688–2701. [PubMed: 18488141]

Sontag JM, Fykse EM, Ushkaryov Y, Liu JP, Robinson PJ, Sudhof TC. Differential expression and regulation of multiple dynamins. J. Biol. Chem. 1994; 269:4547–4554. [PubMed: 8308025]

Stradal TE, Rottner K, Disanza A, Confalonieri S, Innocenti M, Scita G. Regulation of actin dynamics by WASP and WAVE family proteins. Trends Cell Biol. 2004; 14:303–311. [PubMed: 15183187]

Strasser GA, Rahim NA, VanderWaal KE, Gertler FB, Lanier LM. Arp2/3 is a negative regulator of growth cone translocation. Neuron. 2004; 43:81–94. [PubMed: 15233919]

Takei K, Mundigl O, Daniell L, De Camilli P. The synaptic vesicle cycle: a single vesicle budding step involving clathrin and dynamin. J. Cell Biol. 1996; 133:1237–1250. [PubMed: 8682861]

Torre E, McNiven MA, Urrutia R. Dynamin 1 antisense oligonucleotide treatment prevents neurite formation in cultured hippocampal neurons. J. Biol. Chem. 1994; 269:32411–32417. [PubMed: 7798241]

Wachsstock DH, Wilkins JA, Lin S. Specific interaction of vinculin with alpha-actinin. Biochem. Biophys. Res. Commun. 1987; 146:554–560. [PubMed: 3113423]

Weaver AM, Karginov AV, Kinley AW, Weed SA, Li Y, Parsons JT, Cooper JA. Cortactin promotes and stabilizes Arp2/3-induced actin filament network formation. Curr. Biol. 2001; 11:370–374. [PubMed: 11267876]

Yamada KM, Spooner BS, Wessells NK. Axon growth: roles of microfilaments and microtubules. Proc. Natl Acad. Sci. USA. 1970; 66:1206–1212. [PubMed: 5273449]

Yamada KM, Spooner BS, Wessells NK. Ultrastructure and function of growth cones and axons of cultured nerve cells. J. Cell Biol. 1971; 49:614–635. [PubMed: 4326456]

Yamashita T, Hige T, Takahashi T. Vesicle endocytosis requires dynamin-dependent GTP hydrolysis at a fast CNS synapse. Science. 2005; 307:124–127. [PubMed: 15637282]

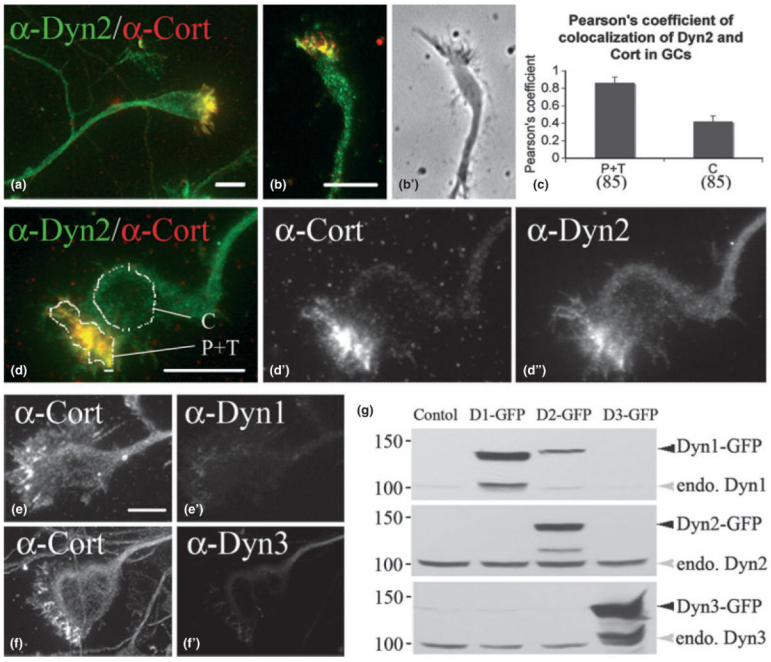

Fig. 1.

Dyn2 and cortactin co-localize in the transitional zone of hippocampal GCs. (a, b, c, and d) Immunofluorescence staining of neurons [Days *in Vitro* (DIV) = 6]. Dyn2 and cortactin are shown in green and red, respectively (a, b, d) (in the figure Cort as short for cortactin). Substantial overlap between the two proteins in the transitional zone and at the base of undulating filopodia was observed. The numbers in brackets represent number of neurons used in the quantitation (c). A white dotted line (d) illustrates a sample 'region of interest' (ROI) for the P zone (composed in this case of the peripheral and transitional zones, P + T on the graph) and central regions (C on graph) used in the Pearson's coefficient calculations of Dyn2/cortactin overlap (c). Co-staining of GCs with Dyn2 and cortactin antibodies, showing localization at the base of motile filopodia as observed by live time-phase microcopy (b, b'). Co-labeling for cortactin and Dyn1 (e, e'), or cortactin and Dyn3 (f, f') showed very little expression of these dynamin forms in GCs. (g) Western blot analysis of HeLa cell lysates expressing Dyn1-GFP, Dyn2-GFP, or Dyn3-GFP to test the specificity of antibodies used in the Immunofluorescence staining (in the western blot D_1 as short for Dyn1, D_2 for Dyn2, and D_3 for Dyn3). Although the Dyn1 reagent had a modest affinity for Dyn2-GFP, neither the Dyn2 or Dyn3 antibodies recognized other variants. Bars = 10 μm.

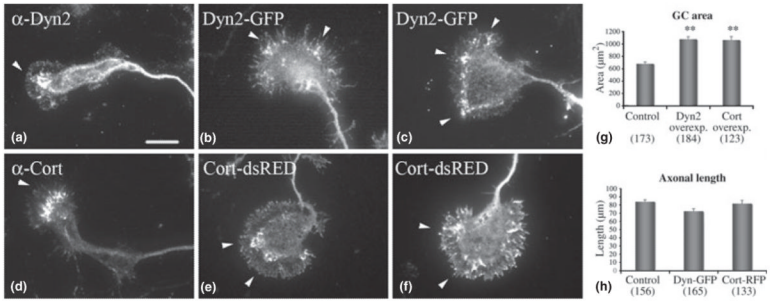

Fig. 2.

Dyn2 and cortactin over-expression induces a marked increase in size and spreading of hippocampal GCs. Immunofluorescence images of control DIV6 neurons stained for Dyn2 (a) and cortactin (d), showing a normal distribution of these proteins in the fan-shaped GC. Over-expression of either Dyn-GFP (b, c) or Cort-dsRED (e, f) in hippocampal neurons leads to a substantial increase in the GC area compared to control GCs (a, d). Adhesion-like punctate structures are distributed around the full periphery of the enlarged extensions (arrowheads). (g) Morphometric analysis of GC size shows 57% and 59% increased sizes for Dyn2-GFP and Cort-dsRED over-expression, respectively, compared with the control. The numbers in brackets represent number of GCs that were measured. (h) Morphometric analysis of axonal length for Dyn2-GFP and Cort-dsRED overexpression and control. Numbers in brackets represent number of axons that were measured. $^{**}p < 0.0001$, bar = 20 μm.

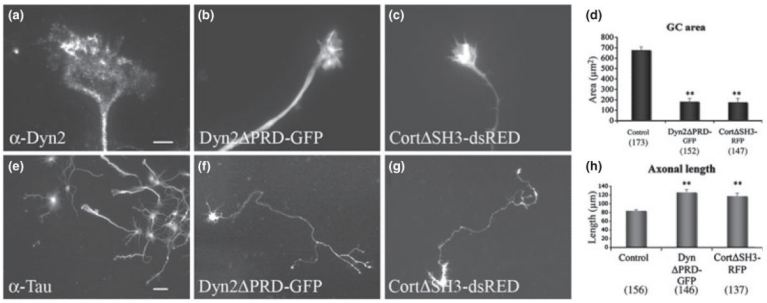

Fig. 3.

Disruption of the Dyn2 and cortactin interaction by expression of truncated proteins results in thin, long axons and small GCs. Immunofluorescence imaging of DIV6 GCs stained for Dyn2 (a) or transfected to express truncated, tagged forms of Dyn2ΔPRD-GFP (b) or CortΔSH3-dsRED (c). Mutant-expressing GCs appear small with long axons compared to those of controls. Morphometric analysis confirms a > 70% decrease in GC area between control (678 μm^2) and mutant-expressing cells (183 μm^2 and 176 μm^2 for Dyn2ΔPRD-GFP and CortΔSH3-dsRED, respectively). Numbers in brackets represent number of GCs that were measured. (d) Lower-magnification images of control neurons stained for tau as a representation of normal axon length in DIV6 neurons (e). (h) A substantial increase in axon length (50% and 39%) from 84 μm (control) to126 μm (Dyn2ΔPRD-GFP) and 117 μM (CortΔSH3-dsRED) is observed for neurons expressing either Dyn2ΔPRD-GFP (f) or CortΔSH3-dsRED. (g) Numbers in brackets represent number of axons that were measured. Error bars are standard error bars, $^{**}p < 0.0001$ (g). (a–c) bar = 10 μm; (e–j) bar = 40 μm.

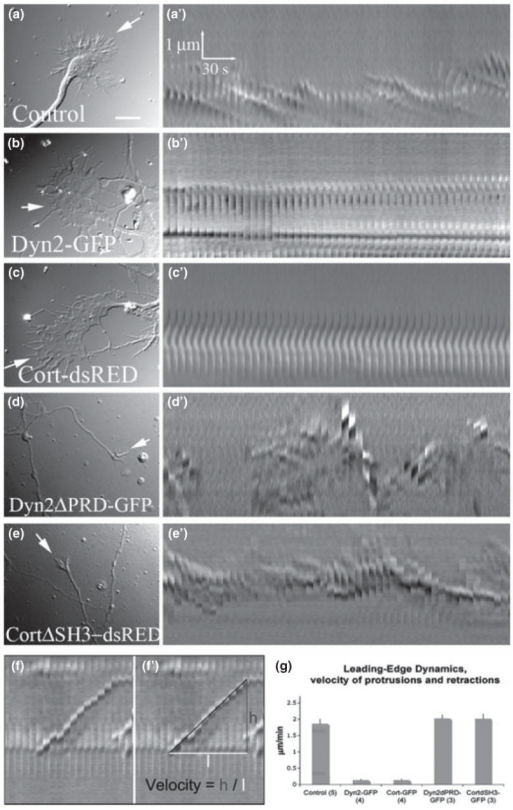

Fig. 4.

Increased expression of Dyn 2 and cortactin influences GC motility. DIC images and corresponding kymographs of DIV6 neurons, either untransfected (a) or transfected to express full-length Dyn2-GFP or Cort-dsRED (b, c) or truncated forms of these proteins (Dyn2ΔPRD-GFP and CortΔSH3-dsRED) in (d, e). Whereas untransfected GCs exhibit normal membrane dynamics and undulations, depicted as sloping lines in the kymograph series (a'), neurons over-expressing Dyn2-GFP (b') or Cort-dsRED (c') possess large, very flat GCs that do not ruffle or move (kymo-graph images are linear). (d', e') Neurons expressing truncated Dyn2/cortactin mutants lacking the interactive PRD/SH3 domains exhibit substantial filopodial ruffling, as depicted in the kymographs. (f, f', g). Quantification of GC dynamics from kymographs shows substantial differences between wt- and mutant-expressing neurons. Numbers in brackets represent the number of kymographs/ cells analyzed. Bar = 40 µM. The scale in b', c', d', e', f, and f' is the same as in a'.

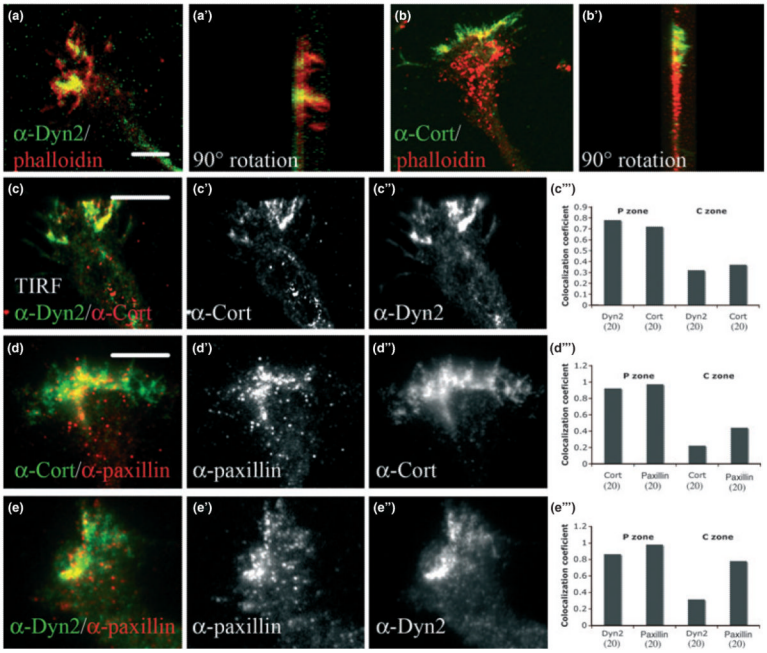

Fig. 5.

Dyn2 and cortactin are components of GC point contacts. Confocal microscopic images of DIV6 GCs co-stained for Dyn2 and Factin (phalloidin) (a) also in supportive movie 6 or cortactin and F-actin (phalloidin) (b) also in supportive movie 7. To define if the regions of overlap (yellow) represent the dorsal or ventral GC membranes, Z-series of GCs were reconstructed to provide an orientation of the protein distribution throughout the GC (a' = 90° rotation of a, b' = 90° rotation of b). Overlapping areas align along the flat edge of the GCs, representing the cover-slip/ventral GC membrane (left side), while the actin-rich filopodia protrude outward from the dorsal surfaces (right side). TIRF microscopy of Dyn2 and cortactin shows that these proteins occupy the very bottom of the GC (c–c'"), where they co-localize considerably, as indicated by the co-localization coefficient (c'"). Both Dyn2 and cortactin co-localize with endogenous paxillin (d–d'", e–e'"), as indicated by the co-localization coefficient (d'" and e'"). Numbers in brackets represent number of GC's that were used in measurements Bars = 10 μm.

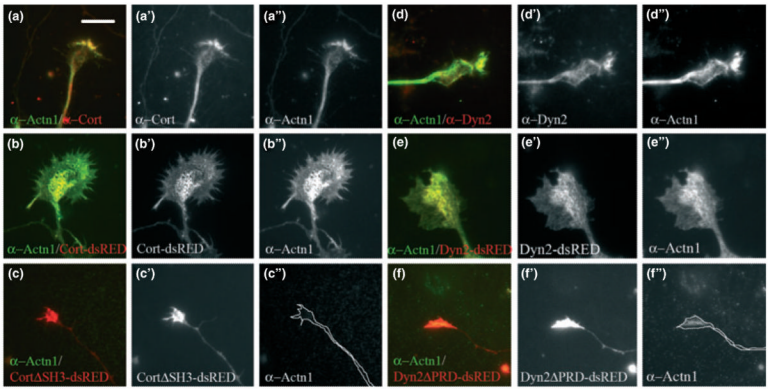

Fig. 6.

Dyn2 and cortactin influence α-actinin1 organization in GCs. Immunofluorescence and TIRF microscopy of DIV4 hippocampal neurons stained for either cortactin (a, a') or Dyn2 (d, d') in red and α-actinin1 (a, a", d, d") (in the figure Actn1 as short for α-actinin1) in green. Over-expression of either Cort-dsRED (b, b', b") or Dyn2-dsRED (e, e', e") in these neurons leads to a substantial increase in the area of α-actinin1 along the base of the GC, as seen by TIRF microscopy. Immunofluorescence imaging of DIV4 GCs expressing truncated, tagged forms of CortΔSH3-dsRED (c, c', c") or Dyn2ΔPRD-dsRED (f, f', f"). Mutant-expressing GCs appear small with negligible amounts of α-actinin1 staining at the base. Bars = 10 μm.

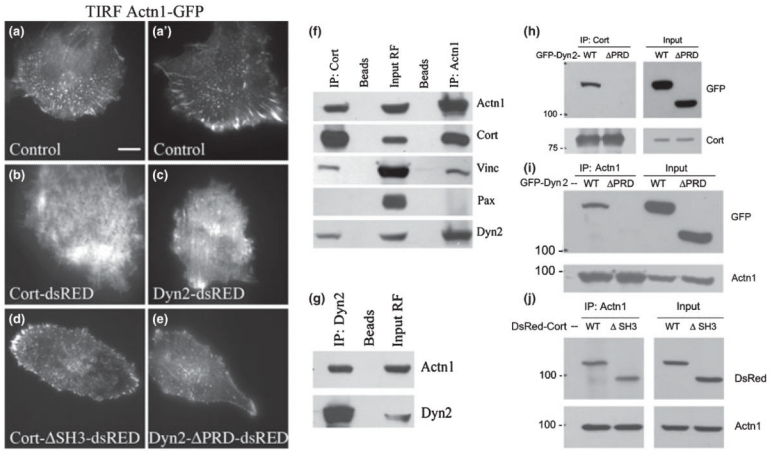

Fig. 7.

Dyn2 and cortactin interact with α-actinin1, resulting in marked recruitment of this complex to the ventral surface. (a–e) TIRF microscopy of rat fibroblasts co-expressing α-actinin1-GFP along with different forms of Dyn2 and cortactin. Cells expressing α-actinin1-GFP alone (a, a') display normal focal adhesion-like structures. In contrast, cells co-transfected to express α-actinin1-GFP with either Cort-dsRED (b) or Dyn2-dsRED (c), redistribute α-actinin1-GFP into an extensive mesh covering the cell base. Cells co-expressing α-actinin1-GFP with either truncated forms of CortΔSH3-dsRED (d) or Dyn2ΔPRD-dsRED (e), show an α-actinin1-GFP distribution similar to that of the control cells, with smaller puncta. (f) Co-IP of cortactin and α-actinin1 complexes from fibroblast lysates probed with antibodies to α-actinin1, vinculin, Dyn2, paxillin, and cortactin. Although control protein A/G beads show no associated proteins, substantial levels of α-actinin1 co-IP with Dyn2 and cortactin. Conversely, an IP for α-actinin1 shows considerable levels of associated Dyn2 and cortactin. Interestingly, these experiments show only modest levels of co-associated vinculin and no paxillin, which are both known proteins of focal adhesions. (g) Co-IP of Dyn2 from cell lysates probed with antibodies to α-actinin1 shows substantial association of the two proteins. (h) Co-IP of cortactin from cells expressing Dyn2-GFP or Dyn2ΔPRD-GFP probed with a GFP antibody. The PRD of Dyn2 is required for interaction with cortactin. (i) IP of α-actinin1 from cells expressing either Dyn2-GFP or Dyn2ΔPRD-GFP. As for the Dyn2-cortactin interaction, the PRD of Dyn2 is required to bind to α-actinin1. (j) A similar experiment to (i) shows an IP of α-actinin1 from cells expressing either Cort-dsRED or CortΔSH3-dsRED, probed with a dsRED antibody. Removal of the SH3 domain from cortactin does not affect the association between the two proteins, suggesting that the interaction is indirect or via another domain of cortactin. (a–e) Bars = 10 μm.